Geometric Modeling of Living Tissue for Subject-Specific Finite Element Analysis

Mitsunori Tada*†, Hiroaki Yoshida*† and Masaaki Mochimaru*†
* Digital Human Research Center, National Institute of Advanced Industrial Science and Technology, Tokyo Japan
† CREST, Japan Science and Technology Agency

***Abstract*— We introduce shape morphing approach to generate subject-specific finite element (FE) models. Different from the conventional approaches, our method generate individual FE model by applying spatial transformation to a reference model. It does not, therefore, require time-consuming works such as segmentation and mesh generation. The proposed method was applied to FE model generation of fingertips. The spatial transformation was computed using volume registration technique. The registration and the FE model morphing were carried out for two subjects. The morphing results showed good agreement in shape both for phalanxes and soft tissue.**

I. Introduction

Finite element (FE) analysis allows us to simulate and predict subcutaneous mechanical behaviors. This method requires time-consuming manual works, segmentation and mesh generation, in advance of the fruitful analysis. An efficient method to generate FE models is crucial for the FE analysis dealing with many subjects. There are two technical challenges in the automation of such method: high-accuracy segmentation and high-quality mesh generation. Various researchers in recent years are trying to overcome these challenges [1], [2], [3].

Thresholding is the most common technique for automatic segmentation. It works well for extracting bone tissues from X-ray CT volume, but it is not appropriate for visually discriminating different compositions of soft tissues. The use of MRI is free from such problem, whereas lowered contrast between tissue and bone is undesirable for the automatic thresholding. Many more advanced segmentation method have been proposed [4], however a fully automated method is yet to be developed.

As for mesh generation, the simplest is to represent the finite element model as a set of voxels [5]. This method requires prohibitively large number of elements to represent detailed local structure. There are several automatic techniques for dividing target area with tetrahedral elements [3]. Although it is preferable to use the hexahedral elements in order to improve the accuracy of the analysis, such a meshing technique that is applicable to the complicated geometries such as a human body is yet to be established.

We intend to conduct finite element analysis for three-dimensional human body both for human study and for product design. At least dozens of individual FE models with precise subcutaneous geometry are required in both analyses. Reproducibility in the anatomical structure and time efficiency in the FE model generation are thus crucial for our purpose. In this paper, we propose a novel method to generate subject-specific three-dimensional FE models. We then apply the proposed method to the FE model generation of fingertip.

II. Method

In this paper, we introduce the shape-morphing approach to generate subject-specific FE models. Different from the conventional approaches that generate FE model of every subject by applying segmentation and mesh generation for the individual volume data, the proposed method generates subject-specific FE model by applying spatial-morphing to a reference FE model.

The reference FE model is carefully generated by manual segmentation and manual mesh generation. MR volume acquisition is performed for target subjects. Spatial mappings that transform the reference geometry into the target geometries are computed by volumetrically registering the target volume to the reference volume. Once the registration is completed, the reference FE model is morphed according to the computed spatial transformations and the FE models for target subjects are obtained.

This method has three advantages over the conventional method: (1) Once the reference FE model is generated in the conventional manner, we can generate FE model of target subjects by applying spatial-morphing to the reference FE model without manual segmentation and manual mesh generation, (2) unlike the similar approaches in the literature [6], [7] where an FE model is simply stretched/shrunk to match the surface geometry, our method takes subsurface geometries into consideration, since MR volume data contains precise subcutaneous information, (3) the resultant FE models are homologous among all subjects: they consist of the same number of elements with the consistent anatomical correspondence.

III. Volume Registraiotn

We use a straightforward extension of Szeliski's spline-based two-dimensional image registration method [8] to the three-dimensional volume registration. In his algorithm, SSD is employed for a similarity measure of two volume data. It is formulated as Equation (1).

$$E_{ssd} = \sum_i \left(V_{target}\left(\boldsymbol{x}_i + \boldsymbol{u}_i\right) - V_{reference}\left(\boldsymbol{x}_i\right) \right)^2 \qquad (1)$$

The displacement is defined at the control vertex assigned in the volume data at regular intervals. Figure 1 shows the

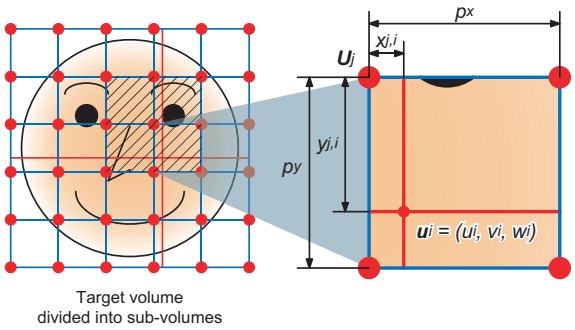

Fig. 1. Displacement spline vertices (filled circle) and sub-volumes (rectangular area bounded by the adjacent control vertices) assigned in the volume data (this figure shows two-dimensional case for simplicity).

distribution of the control vertex. Let us call the rectangular area bounded by the adjacent control vertex as sub-volume. The displacement within a sub-volume is computed by spline approximation from displacements at vertices. The displacement at the i-th voxel $\boldsymbol{u}_i$ is thus obtained from a weighted sum of the displacements at every control vertex,

$$\boldsymbol{u}_i = \sum_j \Omega_{ij} \boldsymbol{U}_j \tag{2}$$

where $\boldsymbol{U}_j = (U_j, V_j, W_j)$ is the displacement at the j-th control vertex and Ω_{ij} is the weight function. In the case when the i-th voxel is within the sub-volume that shares the j-th control vertex (hatched four sub-volumes shown in Figure 1), Ω_{ij} is defined by Equation (3),

$$\Omega_{ij} = (p_x - |x_{j,i}|)\,(p_y - |y_{j,i}|)\,(p_z - |z_{j,i}|)\,/p_x p_y p_z \tag{3}$$

where p_x, p_y and p_z denote the interval between adjacent control vertex in each axial direction, and $|x_{j,i}|$, $|y_{j,i}|$ and $|z_{j,i}|$ denote the distance from j-th control vertex to i-th voxel in each axial direction. Otherwise Ω_{ij} takes zero. In other word, the displacement of i-th voxel is computed by the tri-linear interpolation of the displacement of eight control vertices that compose a sub-volume where i-th voxel exists.

This spline-based transformation model has advantage over a voxel-wise model where the displacement vector is defined at every voxel [9], [10]. The small numbers of DOF reduce computational cost and increase registration stability, while maintaining the versatility of the non-rigid transformation model.

We use the Levenberg-Marquardt method for the minimization of E_{ssd}. A gradient vector and a Hessian matrix of E_{ssd} required for this optimization are approximated from the gradient of the volume intensity as formulated in Equation (4) and (5), respectively,

$$g_j^x = 2 \sum_i \Omega_{ij} E_i G_i^x \tag{4}$$

$$h_{jk}^{yz} = 2 \sum_i \Omega_{ij} \Omega_{ik} G_i^y G_i^z \tag{5}$$

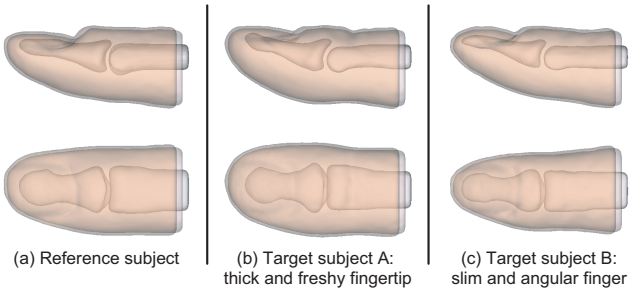

Fig. 2. Iso-surfaces of the segmented MR volume data for three subjects imaged in our experiment.

where, E_i describes the intensity error between the warped target volume and the reference volume, while G_i^x, G_i^y and G_i^z show the spatial gradient in each axial direction. Note that Equation (4) shows only the x component of the gradient vector, while Equation (5) shows only the yz component of the Hessian matrix.

IV. Registration Results

A. Volume Acquisition

We acquired MR volume data of index fingertips of three male subjects aging from 25 to 32. The finger nail of the right hand of each subject was glued to a cylindrical tube that is inserted into a small saddle coil placed at the center of a 4.7 T, 230 mm bore MRI scanner (Unity INOVA, Varian, Inc.). The high magnetic field of this scanner ensured high signal-to-noise ratio of the obtained data. The volume data was obtained with a three-dimensional gradient echo sequence (GE3D) with TR/TE of 20/10 msec, whose field of view (FOV) was 120 $\times$ 30 $\times$ 30 mm and volume size was 512 $\times$ 128 $\times$ 128 voxel. Resolution of the volume data was thus 234 μm/voxel. It took about 5 minutes to obtain a volume data for one subject.

The following four preprocesses are applied to the volume data prior to registration: (1) Trimming the volume data from the middle of the middle phalanx, (2) resizing the trimmed volume data to 256 $\times$ 128 $\times$ 128 so that the finger region is positioned at the center, (3) applying Gaussian filter of 3 $\times$ 3 $\times$ 3 voxel kernel to the resized volume data, and (4) normalizing the smoothed volume data so that the intensity values are scaled into the range of 0.0 to 1.0.

Figure 2 (a), (b) and (c) show the iso-surfaces of the segmented MR volume data for all subjects. Each finger has four surfaces: finger surface, boundary between epidermis and subcutaneous tissue, distal phalanx and middle phalanx. The first subject is call as reference subject, while the latter two subjects are call as target subject A and target subject B for convenience of following explanation. As can be seen in this figure, the joint length of all fingers is approximately the same, while the surface geometries of finger and bones have totally different profiles. Target subject A's fingertip has thick and fleshy shape, while that of target subject B has slim and angular shape. Reference subject has intermediate shape.

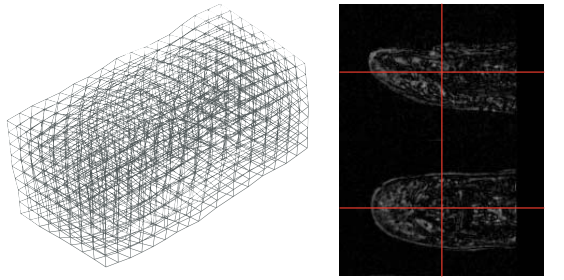

(a1) Spatial transformation (a2) Final difference

(a) Result of volume registration: target subject A to reference subject

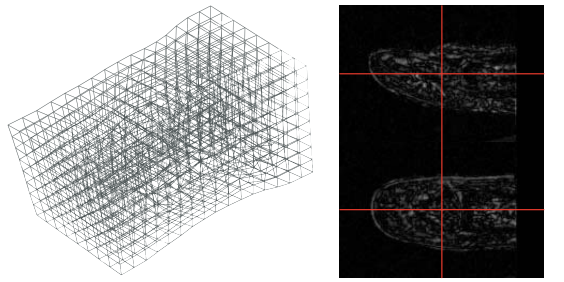

(b1) Spatial transformation (b2) Final difference

(b) Result of volume registration: target subject B to reference subject

Fig. 3. Results of the volume registration.

B. Volume Registration

The registration technique given in Section III was applied to the preprocessed volume data. Reference subject was selected for the reference volume, since he has intermediate surface geometry. Registration was carried out for target subject A to reference subject and for target subject B to reference subject. The intervals p_x, p_y and p_z between the control vertex were set to 16 voxels for each direction. Since the volume data has the voxel size of $256 \times 128 \times 128$, the non-rigid transformation model in this registration has

$$\left(\left(\frac{256}{16}+1\right)\times\left(\frac{128}{16}+1\right)+\left(\frac{128}{16}+1\right)\times 3\right) = 4131 \tag{6}$$

DOF in total. The 4-level Gaussian pyramid was constructed for the coarse-to-fine optimization.

The current implementation takes approximately 160 seconds for completing registration on a Pentium 4 3.8 GHz Windows machine with memory of 2 GB.

Figure 3 shows the results of the registration. Panel (a1) shows the computed spatial transformations for subject A represented as deformed grid, while panel (a2) shows the sagittal and coronal slices of final differences (subtraction between reference subject and target subject after registration). Panels in Figure 3 (b) are the same as that in (a) except that these are for target subject B.

Our registration program succeeded to decrease the intensity error between two volumes. The residual that one can observe in panel (a2) and (b2) are mainly caused due to the individual variation in the texture of the subcutaneous tissue and bone marrow. These textures have higher spatial frequency compared to the size of the sub-volume, and thus they are not matched using the presented algorithm.

V. FE Model Morphing Results

A. Reference FE Model

The spatial transformations computed in Section IV-B allow us to obtain the FE model of the target subjects by morphing the reference FE model that had been generated in the conventional manner.

Creation of the reference FE model requires segmentation of the volume data into four regions. The Sobel filter was applied to each axial slice of the volume data to enhance the boundaries of these regions. Each image was then manually segmented into epidermis, subcutaneous tissue, distal phalanx and middle phalanx referring to the extracted edges. The segmented volume data was retouched in axial, sagittal and coronal directions so that the local irregularities are smoothed. These retouching processes are necessary for obtaining precise geometries from lowered contrast MR volume data. For this purpose, we have developed ancillary software to perform segmentation and retouching.

Next, we create the polygon model of each regions from the segmented data using marching-cube algorithm [11]. The resultant polygon models were imported to Geomagic Studio 8 (Raindrop Geomagic, Inc.) to perform smoothing and NURBS surface generation.

Finally, all the NURBS surfaces were imported to ABAQUS CAE 6.5 (ABAQUS, Inc.) to perform mesh generation. Shown in Figure 4 (a) is the FE model of reference subject generated in this way. The top row and the middle row shows the phalanxes and surface shape of the FE model, while shown in the bottom row is the iso-surfaces of the segmented MR volume data for comparison. This model consists of skin with two layers, distal phalanx and middle phalanx. The thickness of the epidermis was about 0.5 to 0.6 mm that is nearly consistent with the Dandekar's three-dimensional FE model [12]. This reference FE model consists of 106042 tetrahedral elements and 19279 nodes. Good agreements in the shape of finger surface and bones are confirmed. This is not surprising since this model is manually generated.

B. Morphing Reference FE Model to Target

To obtain subject-specific FE models of target volumes (i.e. target subject A and B), we morphed the reference FE model by using the spatial transformations that had been computed in Section IV-B. The displacement of each node was calculated by tri-linear interpolation as formulated in Equation (2). Our method requires only 4 minutes including the execution of the volume registration to obtain subject-specific FE model, while the manual method requires more than 1200 minutes in total.

Shown in Figure 4 (b) and (c) are the results of the FE model morphing to generate FE model of target subject A and target subject B, respectively. Same as Figure 4 (a), the top row and the middle row shows the phalanxes and finger surface of the FE model, while shown in the bottom row is the iso-surface of the segmented MR volume data for comparison.

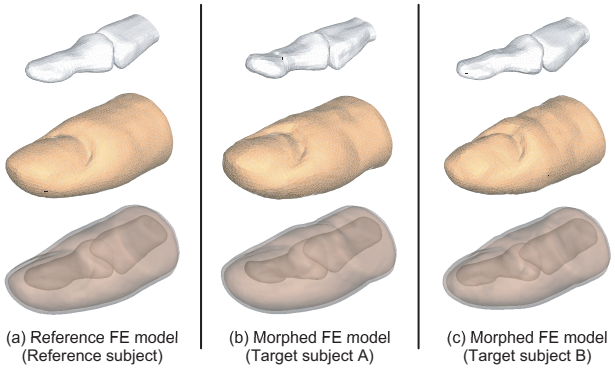

Fig. 4. Results of the FE model morphing, (a) reference model for reference subject, (b) morphed model for target subject A, and (c) morphed model for target subject B.

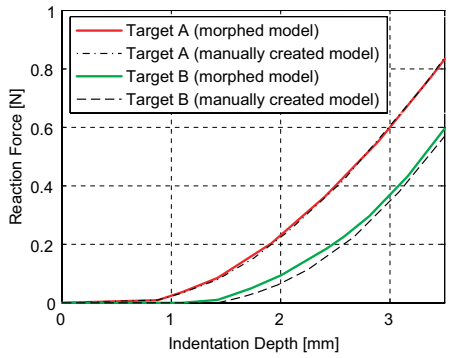

Fig. 5. Computed reaction forces for different FE models.

These are automatically generated FE models that have good agreement in the geometry of finger surface and phalanxes as can be observed in Figure 4. This is because our method has taken subsurface geometry into considerations as well as surface geometries. The ventral sides of fingertips have 0.2 to 0.3 mm error, while the dorsal side and the joint of phalanxes have slightly large error ranging from 0.5 to 0.8 mm. The maximum increase in the aspect ratio of the tetrahedral element due to the FE model morphing was about 20%.

C. Quality of the Morphed FE model

In order to validate the quality of the FE model, morphed FE models and manually created FE models are analyzed under the same condition. FE models of target subject A and target subject B are generated in manual method for this purpose. See Section V-A for detailed procedure of the manual mesh generation. Total number of elements and nodes of these manually generated models are almost the same as those of the morphed models.

The soft tissues and bones were assumed to be linear elastic and isotropic medium. The material constants were determined from the Dandekar's three-dimensional FE model [12]. Both the nail region and surface of phalanxes are fixed. Cylindrical indenter with radius of 5 mm was constructed for the simulation of the uni-axial indentation. The indenter was placed just above the center of the finger pad. There was about 1.0 to 1.5 mm gap between the indenter and the finger pad depending on the surface shape of the fingertip. The indenter moved 3.5 mm downward to indent the finger pad for all models.

ABAQUS 6.5 (ABAQUS, Inc.) was employed to perform FE analysis. Figure 5 shows the results of the analysis. The computed reaction forces for the morphed FE model and for the manually created FE model are almost identical. We can thus conclude that the morphed FE model has enough quality to conduct FE analysis.

VI. Conclusion

We have introduced the shape-morphing approach to generate subject-specific FE models. The proposed method was applied to FE model generation of fingertips. The spatial transformation was computed using volume registration technique based on intensity gradient of MR volume data. The morphing results showed good agreements in geometries both for finger surface and phalanxes. This method dramatically reduces the manual labors in the FE model generation, and is thus considered to be a promising method in FE analysis allowing for the individual shape differences, and dealing with many subjects.

References

[1] J. H. Keyak, J. M. Meagher, H. B. Skinner, and C. D. M. Jr., "Automated three-dimensional finite element modelling of bone: A new method," *Journal of Biomedical Engineering*, vol. 12, pp. 389–397, 1990.

[2] R. Muller and P. Ruegsegger, "Three-dimensional finite element modelling of non-invasively assessed trabecular bone structures," *Medical Engineering and Physics*, vol. 17, no. 2, pp. 126–133, 1995.

[3] B. Merz, M. Lengsfeld, R. Muller, J. Kaminsky, P. Ruegsegger, and P. Niederer, "Automated generation of 3D FE-models of the human femur – comparison of methods and results," *Computer Methods in Biomechanics & Biomedical Engineering*, pp. 125–134, 1996.

[4] L. M. Lorigo, O. D. Faugeras, W. E. L. Grimson, R. Keriven, and R. Kikinis, "Segmentation of bone in clinical knee MRI using texture-based geodesic active contours," in *In Proceedings of International Conference on Medical Image Computing and Computer-Assisted Intervention*, 1998, pp. 1195–1204.

[5] J. H. Keyak, M. G. Fourkas, J. M. Meagher, and H. B. Skinner, "Validation of an automated method of three-dimensional finite element modelling of bone," *Journal of Biomedical Engineering*, vol. 15, no. 6, pp. 505–509, 1993.

[6] B. Couteau, Y. Payan, and S. Lavallee, "The mesh-matching algorithm: an automatic 3D mesh generator for finite element structures," *Journal of Biomechanics*, vol. 33, no. 8, pp. 1005–1009, Aug 2000.

[7] L. Baghdadi, D. A. Steinman, and H. M. Ladak, "Template-based finite-element mesh generation from medical images." *Computer Methods and Programs in Biomedicine*, vol. 77, no. 1, pp. 11–21, Jan 2005. [Online]. Available: http://dx.doi.org/10.1016/j.cmpb.2004.06.002

[8] R. Szeliski and J. Coughlan, "Spline-based image registration," *International Journal of Computer Vision*, vol. 22, no. 3, pp. 199–218, 1997.

[9] B. K. P. Horn and B. G. Schunck, "Determining optical flow," *Artificial Intelligence*, vol. 17, pp. 185–203, 1981.

[10] S. Periaswamy and H. Farid, "Elastic registration in the presence of intensity variations," *IEEE Transactions on Medical Imaging*, vol. 22, no. 7, pp. 865–874, 2003.

[11] W. E. Lorensen and H. E. Cline, "Marching cubes: A high resolution 3D surface reconstruction algorithm," *Computer Graphics*, vol. 21, pp. 163–169, 1987.

[12] K. Dandekar, B. I. Raju, and M. A. Srinivasan, "3-D finite-element models of human and monkey fingertips to investigate the mechanics of tactile sense," *Journal of Biomechanical Engineering*, vol. 125, pp. 682–691, 2003.